Article

Development of broadband underwater radio communication for application in unmanned underwater vehicles

Igor Smolyaninov [1,*], Quirino Balzano [2] and Dendy Young [1]

[1] Saltenna LLC, 1751 Pinnacle Drive, Suite 600 McLean VA 22102-4903 USA;
    igor.smolyaninov@saltenna.com

[2] Electrical and Computer Engineering Department, University of Maryland, College Park, MD 20742 USA;
    qbalzano@umd.edu

* Correspondence: igor.smolyaninov@saltenna.com and smoly@umd.edu

Abstract: This paper presents several novel designs of underwater portable radio antennas operating in the 2 MHz, 50 MHz and 2.4 GHz bands and efficient for launching surface electromagnetic waves at the seawater/air interface. The antenna operation is enabled by an impedance matching antenna enclosure, which is filled with de-ionized water. Enhanced coupling to surface electromagnetic waves is based on the field enhancement at the antenna tip. These design features allow us to reduce antenna dimensions and improve the coupling of electromagnetic energy to the surrounding saltwater medium. Since surface wave propagation length far exceeds the skin depth of conventional radio waves at the same frequency, this technique is useful for broadband underwater wireless communication over distances, which far exceed the skin depth in seawater. We conclude that the developed broadband underwater radio communication technique will be useful in networking of unmanned underwater vehicles.

Keywords: unmanned underwater vehicle; broadband radio communication; surface electromagnetic wave.

1. Introduction

Wide band communication remains the limiting bottleneck for command and control of unmanned underwater vehicles (UUV). Acoustic communication is bandwidth limited due to slow propagation speeds and is susceptible to high error rates due to multi-path effects. Conventional radio frequency (RF) signals have potential for wide bandwidth communications but are severely limited in range due to rapid attenuation in seawater. Directional optical links can provide bandwidth over 200 Mbps in seawater but, until now, have not been successfully integrated into operational UUVs due to the need for sophisticated pointing, acquisition and tracking. In addition, optical links are strongly affected by water turbidity, so that the use of optical wireless communication for reliable UUV-to-UUV links remains highly challenging. Thus, underwater wide bandwidth wireless communication remains a critical technology gap that needs to be filled.

Very recently we have reported a novel design of a surface wave RF antenna operating in the 2.4 GHz band and efficient for launching surface electromagnetic waves at conductor/dielectric interfaces [1]. The antenna operation is based on the strong field enhancement at the antenna tip, which results in efficient excitation of surface electromagnetic waves (SEW) propagating along nearby conductive surfaces. It was demonstrated that this antenna is useful for broadband radio communication through various conductive enclosures, such as typical commercial Faraday cages. It was also hypothesized that a similar design could be used for broadband underwater communication.

Indeed, a successful adaptation of the surface wave antenna design was reported in [2] which operates in the 50 MHz band and is efficient for launching surface electromagnetic waves at the seawater/air interface. In addition to field enhancement at the antenna tip, the antenna operation is based on an impedance matching antenna enclosure, which is filled with de-ionized water [3]. This enclosure allows us to reduce antenna dimensions and improve the coupling of electromagnetic energy to the surrounding saltwater medium. Since surface wave propagation length far exceeds the skin depth of conventional radio waves at the same frequency, this technique is useful for broadband underwater wireless communication over long distances.

In this article we report further development of this concept. We will describe several designs of underwater portable radio antennas operating in the 2 MHz, 50 MHz and 2.4 GHz bands and efficient for launching surface electromagnetic waves at the seawater/air interface. In all cases the developed surface wave underwater antennas are capable of broadband underwater wireless communication over distances which far exceed the skin depth in seawater. We infer that the developed broadband underwater radio communication technique will be useful in communication among unmanned underwater vehicles.

2. Methods

Typically, it is very difficult to establish broadband radio communication through conductive media and enclosures, such as communication through seawater, metallic test chambers, etc. Performance of conventional RF communication schemes in such situations is limited by the very small RF skin depth δ, which may be calculated as:

$$\delta = \sqrt{\frac{1}{\pi \mu_0 \sigma \nu}} \, ,$$

(1)

where σ is the medium conductivity and ν is the communication frequency [4]. In the case of seawater the frequency dependent RF skin depth may be estimated by

$$\delta \approx \frac{270m}{\sqrt{\nu}}$$

(2)

This signal attenuation severely limits the ability to communicate over distance in seawater. For example, at 50 MHz the skin depth in seawater is about 3.8 cm, so conventional techniques of RF communication are impractical over useful distances. In addition, conventional RF signals cannot penetrate through small defects and openings in conductive barriers. For example, the Bethe's [5] expression for the transmission of a conventional TEM wave through a subwavelength aperture is

$$T \propto \left(\frac{a}{\lambda} \right)^4 ,$$

(3)

where a is the aperture size and λ is the free space wavelength. It produces negligible transmission if λ<<a. As a result, conventional techniques of RF communication are also impractical in situations where the walls of an enclosure are conductive.

On the other hand, it is well established that efficient coupling to surface electromagnetic modes which exist at conductor/dielectric interfaces [6] enables efficient signal transmission through continuous conductive barriers (including even metal layers) and through deeply subwavelength apertures in such barriers [7,8]. Following this approach, we have designed a battery-powered 2.45-GHz transmitting surface wave antenna [1], which is capable of sending video signals from inside a -90dB isolation Faraday cage. We believe that this novel capability may be used for remote examination of metal enclosures, as well as improving Wi-Fi connectivity in buildings and underground tunnels. Moreover, a similar surface electromagnetic wave-based approach may be used to achieve broadband RF communication in seawater over distances, which far   exceed the skin depth in seawater [2].

The principle of operation of the surface electromagnetic wave-based antenna is illustrated in Fig.1a. The electromagnetic field of the surface electromagnetic wave is partially longitudinal, which
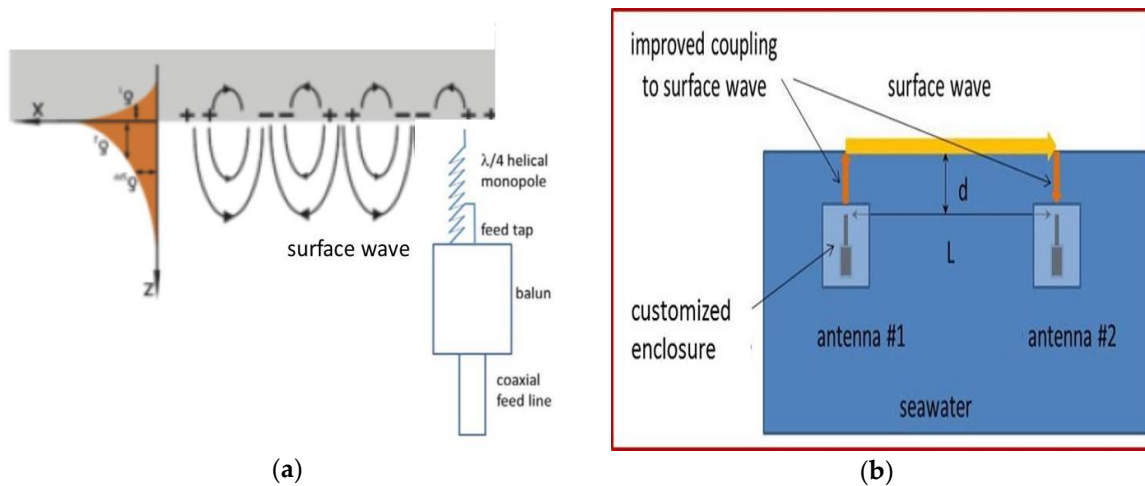
(**a**)   (**b**)

Figure 1. (**a**) Schematic geometry of a 2.4 GHz surface wave antenna design based on helical monopole shorted to its feed line outer conductor. The tip of the antenna is shown near a flat conductive surface where it excites an omnidirectional surface electromagnetic wave. The electromagnetic field of the surface electromagnetic wave is partially longitudinal, which means that an efficient surface wave antenna needs a strong field enhancement at its apex, which "pushes" charges along the metal surface; (**b**) Principle of operation of underwater surface electromagnetic wave RF transmitter

means that a good surface wave antenna needs to be placed in the vicinity of a conductive surface, and it needs a strong field enhancement at its apex, which "pushes" charges along the conductive surface. When such an antenna is adapted for surface wave-based underwater communication, it is encapsulated in an impedance matching antenna enclosure, which is filled with de-ionized water, as illustrated in Fig.1b. This enclosure allows us to reduce antenna dimensions by approximately
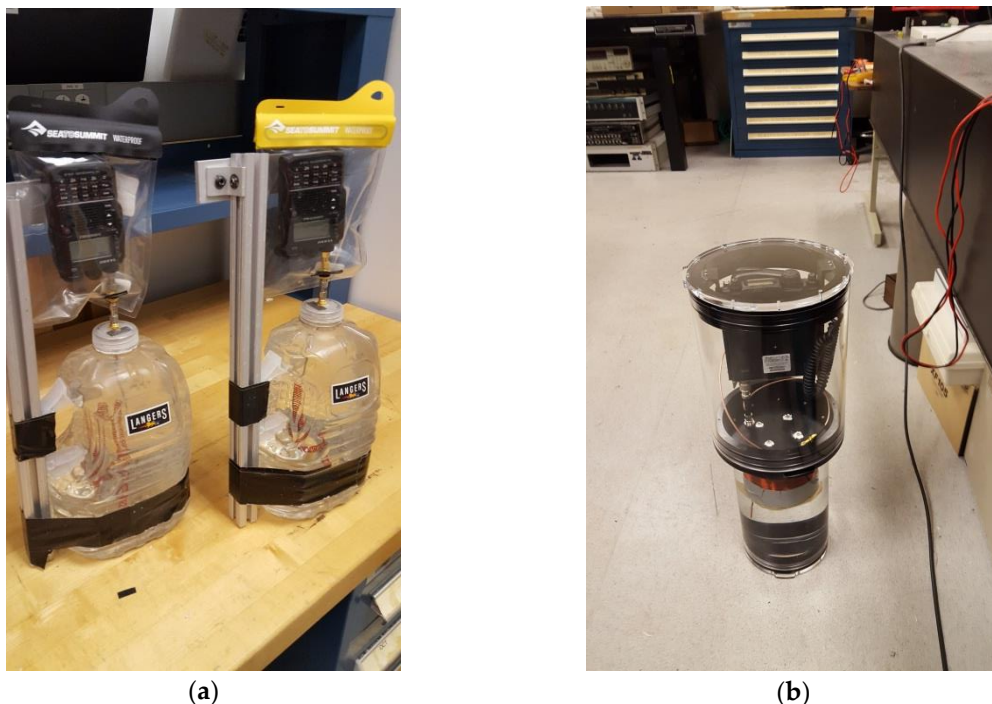

(**a**)   (**b**)

Figure 2. (**a**) Surface wave underwater antennas attached to Yaesu VX-8 radios operated at 50 MHz at 5W output power. The impedance-matching enclosures are filled with de-ionized water; (**b**) Assembled surface wave underwater antenna operating in the 2 MHz band attached to a Yaesu FT-857 radio operated at 5W output power. The impedance-matching enclosure (seen in the bottom section of the assembly) is filled with de-ionized water

factor of 9 compared to free space dimensions, and to improve coupling of electromagnetic energy to the surrounding seawater medium. In addition, it considerably reduces the ohmic losses that would be caused by the immersion of the antenna in saline water. Examples of such antenna designs optimized for operation in the 50 MHz and 2 MHz bands are presented in Fig.2.

A tuning procedure of the surface wave antenna is illustrated in Fig. 3. It shows measurements of S_{11} of the fabricated helical antennas resonant at 2.45 GHz as a function of distance to a large planar copper plane. Depending on the tapping point location, the radiative behavior of the helical antenna may be optimized for either 2D surface wave radiation, or 3D radiation into free space, as illustrated in Fig. 3b. The final tuning of the antenna was performed by maximizing the received video signal outside a closed commercial Faraday chamber, as described in detail in [1].
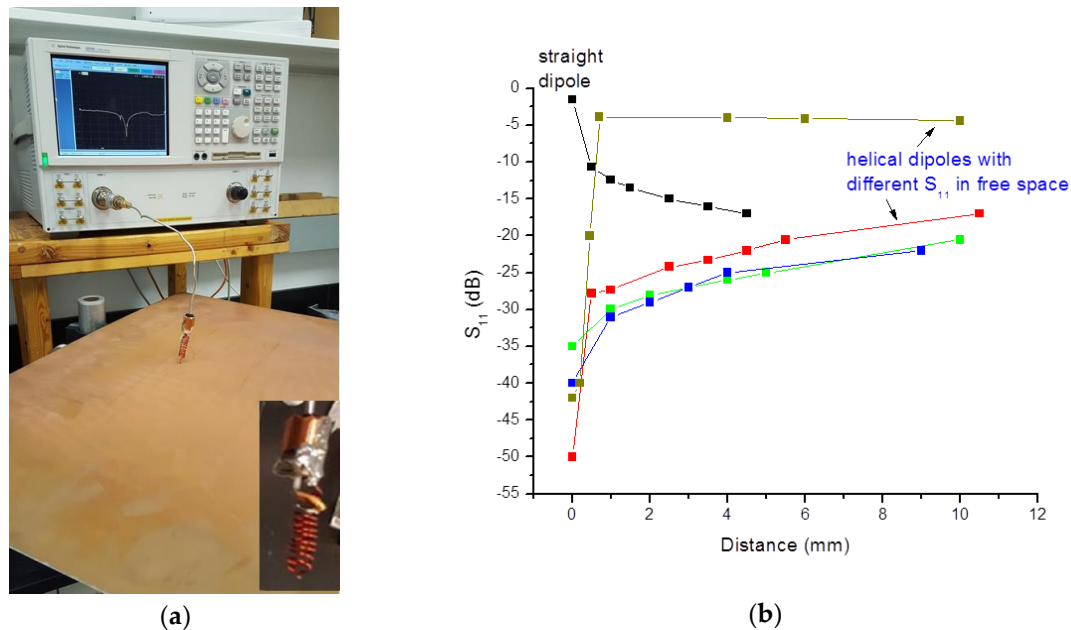

(**a**)   (**b**)

Figure 3. (**a**) Measurements of S_{11} of the fabricated helical antenna resonant at 2.45GHz near a large copper plane. The inset shows a photo of the antenna.; (**b**) Tuning of the fabricated helical antennas resonant at 2.45 GHz via measurements of S_{11} as a function of distance from the large copper plane. The tuning parameter is the tapping point of a feeding coaxial line. Behavior of a conventional dipole antenna is presented for a comparison.

3. Results

3.1. Broadband transmission through Faraday cage

The performance of the surface wave antenna operating in the 2.4 GHz band has been tested by transmitting Wi-Fi video signals through a -90 dB isolation Faraday cage (JRE Test, model 0709), as illustrated in Fig.4. Video signals generated from within the locked Faraday cage and transmitted live through free space without any cabling or connecting ground between the transmitter and receiver were received outside the enclosure and displayed on a live TV monitor. Outside the Faraday enclosure at a distance on the order of 10 to 100 cm, the video signal was received by a similar surface wave antenna.

The SEW-mediated mechanism of 2.4 GHz video signal transmission through the locked Faraday cage has been verified by the transmitted signal measurements near the Faraday cage as a function of distance from the outside wall of the cage [1]. The exponential decay of the transmitted signal outside of the cage confirmed its SEW character. However, the signal received farther away
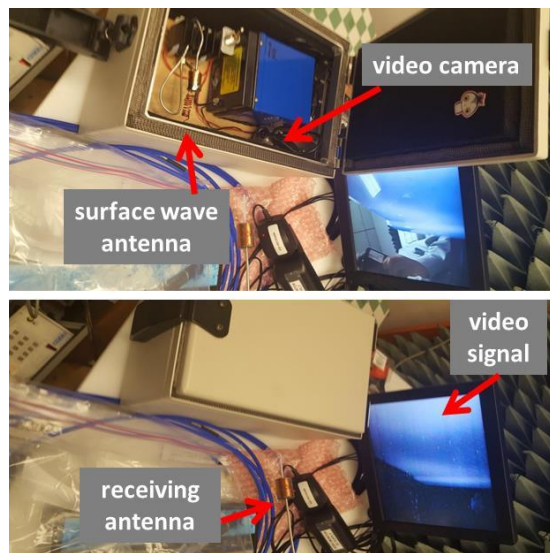
Figure 4. Surface wave antenna keeps transmitting video signal from a locked -90dB Faraday cage.

from the cage (in the far field zone) originated from the transmitted SEW field reaching the cage corners and scattering into the conventional propagating TEM fields.

3.2. Broadband underwater RF communication experiments in laboratory settings

It is obvious that the experiments with a Faraday cage depicted in Fig.4 above are topologically equivalent to the experiments with the same 2.4 GHz SEW antennas performed in a seawater aquarium, which are depicted in Fig.5. In these experiments the seawater surrounding the Wi-Fi video transmitter (which is enclosed in a watertight plastic case) plays the role of a Faraday cage.

(**a**)   (**b**)

Figure 5. (**a**) Similar to experiments depicted in Fig.4, a 2.4 GHz surface wave antenna transmits video signal from inside an aquarium filled with seawater; (**b**) The video transmission is not affected by water turbidity.

Note that the skin depth of seawater at 2.4 GHz is 3 mm, while the thickness of seawater layer around the watertight plastic case was at least 15 cm on each side. Note also that water turbidity did not affect video signal transmission, as illustrated in Fig.5b. Thus, similar to transmission through a Faraday cage, the SEW antenna clearly demonstrates increased capacity for Wi-Fi transmission through seawater. This increased capacity may be understood based on the theoretical values for SEW propagation length L_r along the seawater-air interface, and the penetration depth L_z of SEW field into the seawater [2]. Based on the detailed theoretical consideration in [6,9], they are given by the following expressions:

$$L_z \approx \frac{\lambda_0}{4\pi\sqrt{\varepsilon''}} \quad, \tag{4}$$

and

$$L_r \approx \frac{\lambda_0 \varepsilon''}{\pi} \quad, \tag{5}$$

respectively [4], where ε″ is the imaginary part of the dielectric constant of seawater and λ_0 is the free space wavelength. For example, at 50 MHz the SEW propagation distance appears to be rather large (L_r = 60 m), while (assuming operation down to –90dB relative signal levels) the communication depth may reach several meters. These distances appear to be much larger than the 3.8 cm skin depth of seawater at 50 MHz. This argument is illustrated in Fig.6, which shows the RF field distribution in seawater produced by a point source located in the vicinity of the seawater/air interface. At some distance from a source (which is much longer than the bulk skin depth of seawater) the field distribution is dominated by the surface electromagnetic wave, which enables RF communication from point A to point B, which would otherwise be impossible in the absence of the surface electromagnetic wave.
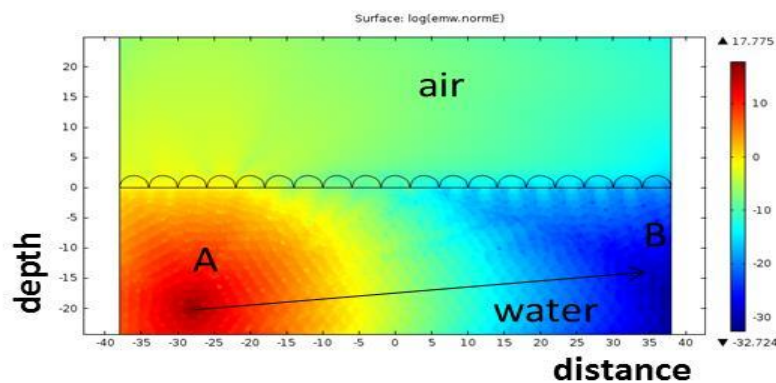

Figure 6. Numerical simulations of RF field distribution in seawater produced by a point source located in the vicinity of the seawater/air interface performed using the COMSOL Multiphysics solver. At some distance from a source the field distribution is dominated by the surface electromagnetic wave.
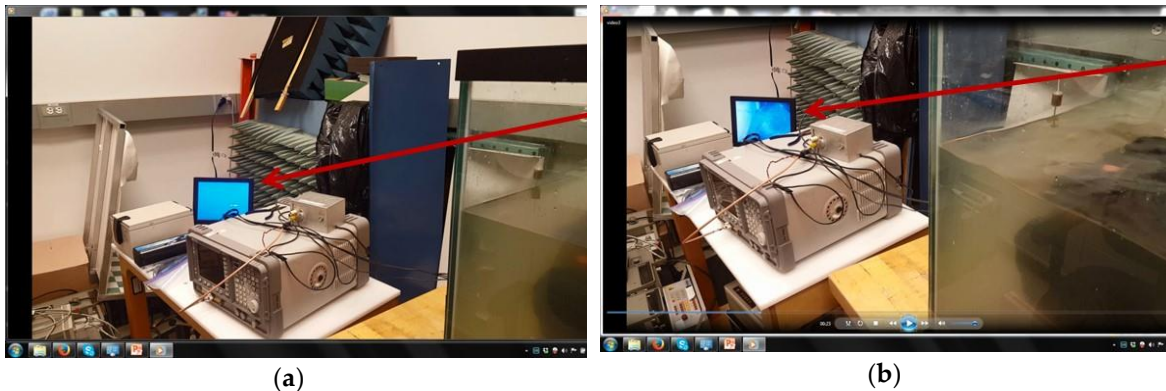

(**a**)   (**b**)

Figure 7. (**a**) The Wi-Fi underwater video transmitter is moved beyond the free space communication range in a seawater aquarium with still water surface; (**b**) The video link is re-established when the seawater surface is agitated.

We should also note that waviness of the seawater-air interface may further promote coupling of the electromagnetic energy into the SEW modes. Such an increased coupling is well established in the closely related field of plasmonics [6], and it was observed in our model experiments performed in a seawater aquarium at 2.4 GHz (see Fig.7). These simple experiments indicate that an agitated sea state may not necessarily present a problem for SEW-based broadband underwater RF communication.

Directionality of SEW beams, which is also well known in plasmonics [6,10] may further improve performance of underwater RF communication links, since it may to some extent alleviate deterioration of link performance due to high propagation losses in seawater. We were able to demonstrate directional excitation and propagation of SEW waves in model experiments performed in a freshwater aquarium in laboratory settings, as illustrated in Fig.8.
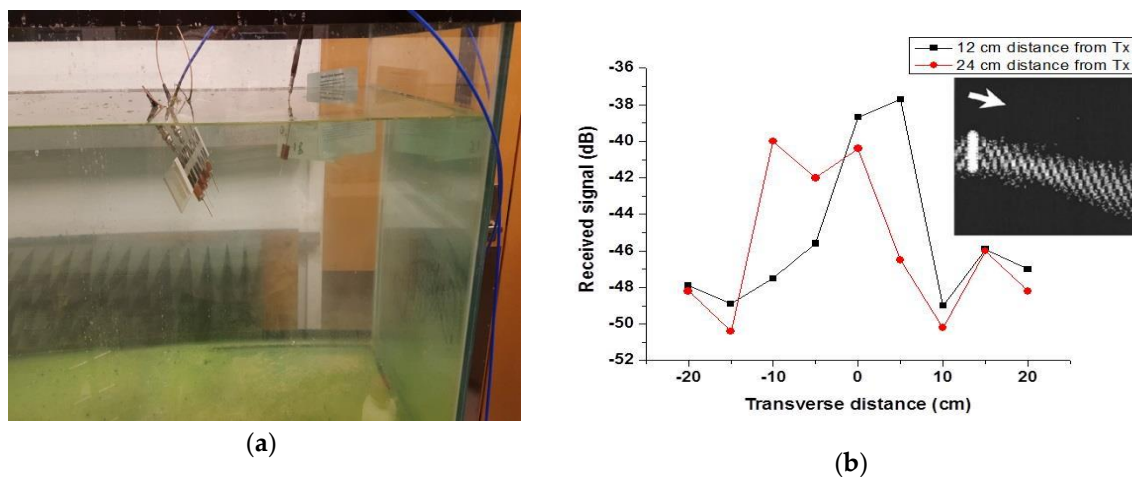

(**a**)

(**b**)

Figure 8. (**a**) 400 MHz SEW field of an antenna array submerged into a fresh water aquarium is probed by a distant dipole receiver; (**b**) Antenna array field measured in the transverse direction at 12 cm and 24 cm from the array. The inset shows numerical modeling of SEW directional beaming from the antenna array.

In these experiments we have used an array of four dipole antennas spaced at 5 cm distances, which resonate at 2.4 GHz in air. After the array was submerged into a freshwater aquarium, its resonant frequency shifted to 400 MHz. The antenna array field was probed by a distant dipole receiver identical to individual antennas in the array, as illustrated in Fig.8a. It was verified that there was no relevant coupling between the feed lines above water. The antenna array field measured in the transverse direction at two distances from the array is plotted in Fig.8b, which also shows our numerical modeling of SEW beaming.

3.3. Field testing of broadband underwater RF communication

The operational performance of the surface wave antennas described above has been tested in an underwater, saline environment near Panama City, Florida (average water salinity 3.0%) [2]. The operating frequency was 50 MHz. The seawater environment was large enough, so that no significant boundary effects were present. All the tests were conducted with separate battery-operated transmitting (TX) and receiving (RX) antenna and radio systems enclosed in watertight containers (shown in Fig.2a) which were handled by divers, as illustrated in Fig.9a. The divers verified their depth and distance using fixed markers made of buoys and ropes. Signal propagation data read from the LED indicator and the S-meter of the Yaesu radios were reported by the divers and recorded by test personnel located on a nearby vessel. The averaged measured values of link probability are plotted in Fig. 9b. The skin depth at 50 MHz in seawater (3.8 cm) is shown near the bottom left corner of the plot for comparison.   These results clearly demonstrate that the novel underwater SEW antennas described above enable RF

communication range/depth combinations which far exceed the known skin depth of seawater. Relatively large variations of the link probability observed in our experiments may be attributed to the variations in the sea surface wave ripples and salinity during the measurements.
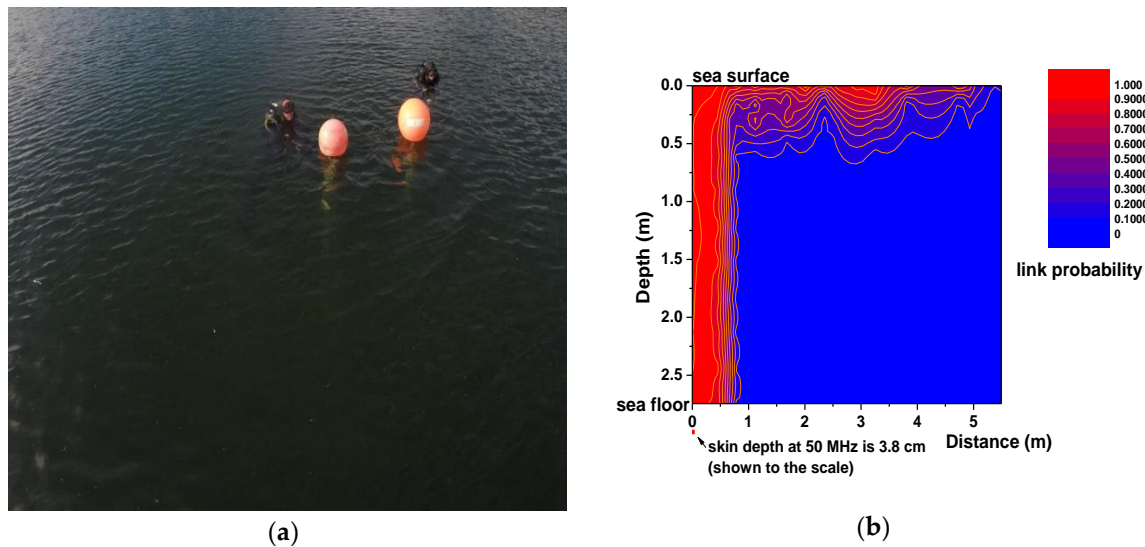

(**a**)   (**b**)

Figure 9. (**a**) Photo of the surface of the actual under water test range.; (**b**) Contour plot of the link probability as a function of depth/distance combination measured in seawater. The sea floor in these experiments was located at 9 m depth. The skin depth in seawater at 50 MHz is shown to the scale for comparison.

Table 1. Summary of the theoretically predicted propagation range Lr and communication depth Lz (@ 5W transmit power) at the RF bands explored in this paper.

	2.4 GHz band	**50 MHz band**	**2 MHz band**
Lz	0.054 m	0.7 m	3.5 m
Lr	3.8 m	60 m	900 km [1]

[1] Theoretical numbers given by Eq.(5) may not be reliable in this band due to Earth curvature.

While the observed SEW signal propagation at 50 MHz was considerably below the theoretically projected L_r=60 m, we expect that further optimization of the antenna parameters will result in reaching the theoretical performance depth/distance limits described by Eqs. (4,5). These performance limits are summarized in Table 1 for the set of RF bands explored in this paper. Note that predictions given by Eq(5) may not be reliable at smaller frequencies due to the fact that it was derived for a planar conductor-dielectric interface.

4. Discussion and Conclusions

The communication distance/depth combinations summarized in Table 1 provide quite an optimistic outlook for potential applications of SEW antennas in underwater communication between divers and UUVs, since even larger communication depth may be achieved at lower frequencies. For example, it appears that L_z~15 m is achievable in the 0.1 MHz band at quite modest 5 W transmit power. Our experimental and theoretical results appear to be novel and important, since until now it was generally believed that broadband radio communication through seawater is impossible over any practically meaningful distance. We expect that further optimization of the antenna parameters will result in approaching the theoretical performance depth/distance limits described by Eqs. (4,5), which will enable novel capacity for wide bandwidth RF signal transmission through seawater, while reducing the power requirements, weight and size of the transmitting and receiving units. We should also note that our SEW-based RF communication scheme should be able to breach the seawater barrier for UAV to UUV communication, since the surface wave EM field is present both above and below the seawater surface. This would enable, for example, a drone

skimming the surface of the water to pick up the electronic transmissions coming from a UUV. The described antennas may also be made multi-spectral so that the communication bandwidth at a given distance/depth combination may be optimized under software control, shifting to larger bandwidths over shorter distances. Our communication scheme may also find applications in frogman to frogman communication, underwater object detection, UUV swarming and mesh networked UUVs, offshore oil platforms, etc. We also expect that our work will result in considerable improvement of Wi-Fi connectivity in buildings, underground tunnels, as well as remote examination of metal and partially metal enclosures, such as shipping containers, metallic test chambers, etc.

Conflicts of Interest: The authors declare no conflict of interest

References

1. Smolyaninov, I. I.; Balzano, Q.; Young D. Surface wave-based radio communication through conductive enclosures. *PIER M* **2019**, *85*, 21-28.
2. Smolyaninov, I. I.; Balzano, Q.; Davis, C. C.; Young, D. Surface wave-based underwater radio communication. *IEEE Antennas and Wireless Propagation Letters*   **2018**, *17*, 2503-2507.
3. Smolyaninov, I. I. Communication and sensor techniques for underwater radio communication, US Patent Application Publication # US 20180198536 (7/12/2018).
4. Cheng, D. K. Fundamentals of Engineering Electromagnetics. Pearson, London, UK, **1992**. Chapter 8.
5. Bethe, H. A. Theory of diffraction by small holes. *Phys. Rev.* **1944**, *66*, 163.
6. Zayats, A. V.; Smolyaninov, I. I.; Maradudin, A. Nano-optics of surface plasmon-polaritons. *Physics Reports* **2005**, *408*, 131-314.
7. Ebbesen, T. W.; Lezec, H. J.; Ghaemi, H. F.; Thio, T.; Wolff, P. A. Extraordinary optical transmission through sub-wavelength hole arrays. *Nature* **1998**, 391, 667-669.
8. Elliott, J.; Smolyaninov, I. I.; Zheludev, N. I.; Zayats, A. V. Polarization control of optical transmission of a periodic array of elliptical holes in a metal films. *Optics Letters* **2004**, 29, 1414-1416.
9. Michalski K. A.; Mosig, J. R. The Sommerfeld half-space problem revisited: from radio frequencies and Zenneck waves to visible light and Fano modes. *Journal of Electromagnetic Waves and Applications* **2016**, 30, 1-42.
10. Smolyaninov, I. I.; Mazzoni, D. L.; Davis, C. C. Imaging of surface plasmon scattering by lithographically created individual surface defects. *Phys. Rev. Letters* **1996**, 77, 3877-3880.